VITAL RATES FROM THE ACTION OF MUTATION ACCUMULATION

KENNETH W. WACHTER, DAVID R. STEINSALTZ, AND STEVEN N. EVANS

Abstract. New models for evolutionary processes of mutation accumulation allow hypotheses about the age-specificity of mutational effects to be translated into predictions of heterogeneous population hazard functions. We apply these models to questions in the biodemography of longevity, including proposed explanations of Gompertz hazards and mortality plateaus, and use them to explore the possibility of melding evolutionary and functional models of aging.

1. Mutation Accumulation

Why are flies, worms, and humans subject to laws of age-specific adult mortality that are uncannily similar in shape? After suitable species-specific changes in scale, organisms with different environments, life histories, body plans, and lifespans turn out to resemble each other in the statistics of their demise. Similarities are typically expressed in terms of hazard functions. The hazard function is a summary measure of rates of death by age across a population, equal to the negative slope of the logarithm of the population survivorship function. Hazard functions for populations from many species show two of the same features, exponential increase with age over a stretch of ages and attenuated increase over later ages generating the visual appearance of a plateau. Discovery and quantification of these commonalities have been signal achievements of the new biodemography, summed up by Vaupel et al. (1998), Carey (2003), Wachter and Finch (1997), and Tuljapurkar (2003).

Explanations for shared features of senescent mortality across species are sought in considerations from reliability engineering, from optimal life-history theory, and from evolutionary processes of antagonistic pleiotropy and mutation accumulation. The first is a *functional* approach to senescence, picturing the organism as a machine with some component structure, attempting to derive the failure modes of the whole from some presumably simpler failure modes of the components. The aim is usually to draw inferences from qualitative classes of structures to general shapes of mortality curves. The enterprise is considered successful if the broad features common to many real-world mortality rates are reproduced in the model. Some examples are Strehler and Mildvan (1960), Rosen (1978), Gavrilov (1978), Gavrilov and Gavrilova (1991), Weitz and Fraser (2001), and Finkelstein and Esaulova (2006).

The other listed approaches are teleological, seeking in different ways to reverse-engineer the physiology of aging in terms of the pseudo-purposeful action of natural

Date: August 26, 2008.

1991 *Mathematics Subject Classification.* 92D15, 37N25, 92D10.

Key words and phrases. evolution, genetic load, senescence.

This work has been supported by Grant AG-P01-008454 from the U.S. National Institute on Aging, and the research of the third author has been supported in part by Grant DMS-0405778 from the U.S. National Science Foundation.

selection. Functional models start from the structure of the organism, while evolutionary models pose prior questions: What kind of machine is the organism, and why is it put together the way it is? Many functional models lead to the same general pattern for mortality rates, after all, and each generic class of models can yield diverse shapes of age-specific mortality. Optimal life-history approaches try to narrow down the choices *a priori*, by explaining why a given structural framework, or a certain choice of parameters within the structural framework, might be evolutionarily preferred. Much work in this area (for example, Rose (1985), Schnebel and Grossfield (1988) Hedrick (1999), Wachter (1999), Williams and Day (2003)) builds on the concept of *antagonistic pleiotropy*, introduced into the theory of senescence by Williams (1957). Williams held that early reproduction and late survival would be negatively linked through direct genetic mechanisms. Recent research often abstracts from the genetic term "pleiotropy", to contemplation of more general trade-offs and compromises that operate across time within the lifetime of an organism and across generations (cf. Toupance et al. (1998), Hasty (2001), Campisi (2003), and Nystrom (2003)).

The other side of the conventional evolutionary theory of aging, called *mutation accumulation*, views senescence not as an optimal trade-off between early- and late-life reproductive success, but rather as the age-specific effect of genetic load, a concept developed by Medawar (1952). Ongoing random mutation spews mostly deleterious changes into the genome. Since the only genetic "repair mechanism" is the death of the organism carrying the defect, there is perpetually an overhang of deaths not yet realized, stretching from the time of the initial mutation until all descendants have died from the effect of the allele. Less nocive mutations linger. Since an individual may not live long enough to experience the harm from a late-acting mutation, this provides another process through which natural selection reshapes demographic schedules. At equilibrium, mortality rates trend upward with age in proportion to the weakening force of selection. The population observed at any given time will be found to be genetically heterogeneous, because new mutations with particular age effects are scattered independently across the individuals in a population and the mutations act together to alter each individual's internal susceptibilities to causes of death.

All these considerations presumably contribute to a general phenomenon, that risks of impairment and death rise with age. None excludes the others. In this article, we concentrate on mutation accumulation, but in a way that begins to illustrate how the evolutionary perspective might be linked to mechanistic and physiological models. Of course, it is easy to recognize that the trade-offs and age-specific mortality impacts must be embodied in complex reliability structures, but the mathematical development on both sides had lacked the flexibility that would be required of a more synoptic model, Pletcher and Neuhauser (2000) being one notable exception.

Reliability models such as that of Gavrilov and Gavrilova (2001) typically posit an underlying structure of components which do not age, that is to say, which are subject to failure times from an exponential probability distribution. The models go on to identify death with the failure of the first component to fail, or with the failure of some specified subset of components. To set such models into an evolutionary context we would want to allow the structure to evolve in some plausible fashion, or to model a genetic modification of the mortality effect of failed components. In

such a way, each perspective could begin to resolve the arbitrariness from which the other suffers.

We take up this challenge in the context of mutation accumulation. Decades of research have piece by piece established a mathematical framework for characterizing genetic load and the interplay between mutation, selection, and recombination. Developments through the end of the Twentieth Century are presented in an authoritative book by Bürger (2000). Early achievements addressed single locus and several locus systems with rich genetic structure, but did not attempt to superimpose demographic dimensions. Charlesworth (1994) succeeded in consolidating an age-specific demographic treatment based on a linear approximation. Charlesworth (2001) showed that both of the tell-tale common features of hazard functions across species, the exponential Gompertzian rise and the eventual onset of plateaus, could be predicted by the linear approximate model from simple, minimalist assumptions. His ideas have attracted wide attention.

There are two crucial obstacles that block the path to a broader application of mutation-accumulation models: first, the limited versions of age-specific genetic harm considered in most research to date; and second, the assumption that genetic loci affecting different age ranges evolve independently. The earliest work of Hamilton (1966) imagined mutations that apply a single bolus of mortality at one fixed age, what we call the "point-mass" model. Charlesworth (2001) allowed for a few other stylized patterns of effect: Mortality increase in a fixed window, in a Gaussian shape around a fixed center, or stepwise increase in mortality starting at a fixed age. A hypothetical mutant allele that changed the reliability structure, whether by modifying the number or type of components or their interactions, would fall outside this framework in both respects: The induced change in mortality rates would be distributed in a complex way across ages; and distinct mutations would not evolve independently, since their effects would interact. Notice (and this is an essential feature of demographically-based models) that the evolution at distinct sites fails to be independent *even if they act independently*; that is, even if the mortality increment due to both alleles co-occurring is simply the sum of their individual effects. To put it simply, death comes to an individual only once, so that any mutation that increases mortality makes a second mutation that also increases mortality less costly, as measured in lost reproductive opportunity.

It might be argued that linearization — the method employed by Brian Charlesworth and others to treat multiple mutations as though they were evolving independently — provides reasonable first approximations to the truth, and is appropriate in models such as these, whose details are considered to be more illustrative than literally true. In fact, though, as has been shown in Steinsaltz et al. (2005) and Wachter et al. (2008), a full nonlinear treatment of even the point-mass case yields qualitatively different outcomes than the linearized simplification. While each single mutant allele in this model has infinitesimal effects — the bedrock of linearization — the premise of mutation accumulation as an explanation for senescence is that the total effects of these individually insignificant mutations accumulate to effective levels; the very point at which the model becomes relevant is the point at which the linearization breaks down, because interactions among age groups can no longer be neglected. For similar reasons — as discussed at length in Wachter et al. (2008) — the distribution of mortality effects within and between different mutations can be decisive.

In this paper, we take a small step toward incorporating physiological mechanism into mutation selection, one which at the same time links backward to earlier work on point-mass mutation models. In our model here, mutant alleles arise that independently increase mortality rates according to the profile of a Gamma density function — a standard element of reliability models — but with additive cumulative effects. We show that the features of prime interest, Gompertzian stretches and late-age plateaus, can be produced within this family, with a range of choices of specific parameter values. These Gamma-distribution mortality profiles are approximately the kind of mutational effect one would expect if the "essential organs" of Gavrilov and Gavrilova (1991) were replaced by a large number of "useful organs", of similar internal redundancy, whose propensity to failure were triggered, or exacerbated, by the presence of one or more mutant alleles. The analogy is not exact, to be sure, as the Gamma-profile corresponds only approximately to the impact of changing the redundancy structure or failure rates of components. This version has the advantage of simplicity of description and analogy to the older point-mass models. At the same time, it is complex enough to illustrate many of the key features of the general mutation-selection models that could be applied to any underlying structural model that an interested reader might care to pursue. We will address accumulation of mutations affecting component redundancy within a reliability model in a later paper.

2. The general mutation-selection model

Medawar's idea of mutation accumulation as a cause of senescence depends upon the action of large numbers of mutations, each with small deleterious effects on survival at specific ranges of age. Mutations which affect young ages are weeded out of the population quickly by natural selection, because members who carry them contribute fewer offspring to the next generation. Mutations affecting older individuals with less remaining reproductive potential to lose are weeded out less rapidly. While weeding is going on, new mutations are being introduced at random into the population. Mutant alleles accumulate until a balance is reached between the force of mutation and the force of selection. All things being equal, the less costly mutations — those that produce their harm later — will be more common at equilibrium.

We outline here the basic mathematical model developed in Steinsaltz et al. (2005), Evans et al. (2007), and Wachter et al. (2008). This is an individual-gene model, not a quantitative genetics model. The accumulating mutations under study here are germ-line mutations maintained in the genome over long stretches of evolutionary time. The general framework of these papers may also have some application to somatic mutations accumulating in individual organisms across the lifecourse, but that is not the focus in the current paper.

Our models are infinite-population models with large or infinite numbers of genetic loci, in the tradition of a famous paper by Kimura and Maruyama (1966). We posit a set $\mathcal{M}$ of potential mutations, which may be finite or infinite. If it is infinite, it must be fitted with a geometric structure, to allow us to describe the process of picking a new set of random mutations which are passed on to the next generation. Description of the model includes a rate measure ν — a function describing the rate at which different mutations from $\mathcal{M}$ arise — and a selective cost function S, quantifying the genetic load imposed by a given collection of mutant alleles.

There is also a related function which translates a collection of mutant alleles into an individual mortality profile. Beyond this there is no attempt to identify alleles with genes on chromosomes, or otherwise to model biological structures. Versatile age-specific structure is achieved in conjunction with some degree of stylization in the representation of the genome.

For mathematical details we refer the reader to the paper Steinsaltz et al. (2005) (for the version excluding genetic recombination) or Wachter et al. (2008) (for the "Free Recombination" version, in which recombination operates on a more rapid time scale than mutation and selection). Our two treatments of recombination bracket a potential continuum of more complex treatments. In each case, there are analytic solutions available to describe the entire time trajectories of the population. In this paper, we will be concerned primarily with equilibrium states. Equilibrium states are distributions of genotypes which are stable in time, under the joint action of mutation and selection. In many situations, there is a unique equilibrium state, and this represents the distribution to which the population converges over time.

We introduce a flexible family of examples in Section 3 and show what goes into its specification and what comes out in the way of predicted hazard functions. We describe the mortality outcomes predicted by the formal theory in Section 4. The goal is to situate a rudimentary kind of reliability model in a mutation-accumulation context, adumbrating a more sophisticated melding of these conceptually divergent approaches. The evolutionary unified failure theory of our aspiration would need to incorporate elements of optimal life history, as well as accounting for the complex hierarchy of trade-offs, from the level of single genes and organelles up to ecosystems, and on timescales from the milliseconds of RNA transcription to the millennia of evolutionary time.

3. Profiles for Mutational Action

In order to calculate predictions in any given case, we need to describe the age-specific effects of mutant alleles, the mutation rates at which alleles enter the population, and the selective cost function which translates the age-specific effects into rates at which alleles are steadily being lost from the population.

In the present work, we identify the mutation space $\mathcal{M}$ with the real numbers greater than one. The effect of allele m is assumed to be the addition of an increment $\eta(m)\kappa(m,x)$ onto the *cumulative* hazard function at age x.

Here we take the profile $\kappa(m,x)$ to be the cumulative distribution function for a shifted Gamma probability distribution. The Gamma shape parameter equals the index value m and varies from allele to allele. The Gamma rate parameter ϕ is the same for all alleles. The shift α for the origin is the age of maturity; alleles only affect adult mortality. Each effect is assigned an effect size $\eta(m)$ which adjusts the strength of the action.

In addition to their association with reliability models, Gamma distribution functions offer advantages of familiarity and flexibility. They offer a clear contrast to the point-mass profiles going back to W. D. Hamilton already studied in Wachter et al. (2008). In the point-mass setting, $\kappa(m,x)$ is a unit step-function and m indexes the age at the step. In our present setting, higher values of m still correspond to later-acting alleles, but effects are spread across ages, with wider spread for later-acting alleles. Even late-acting alleles have some small effect at young adult ages, a salient difference from the point-mass case. The more the mutational

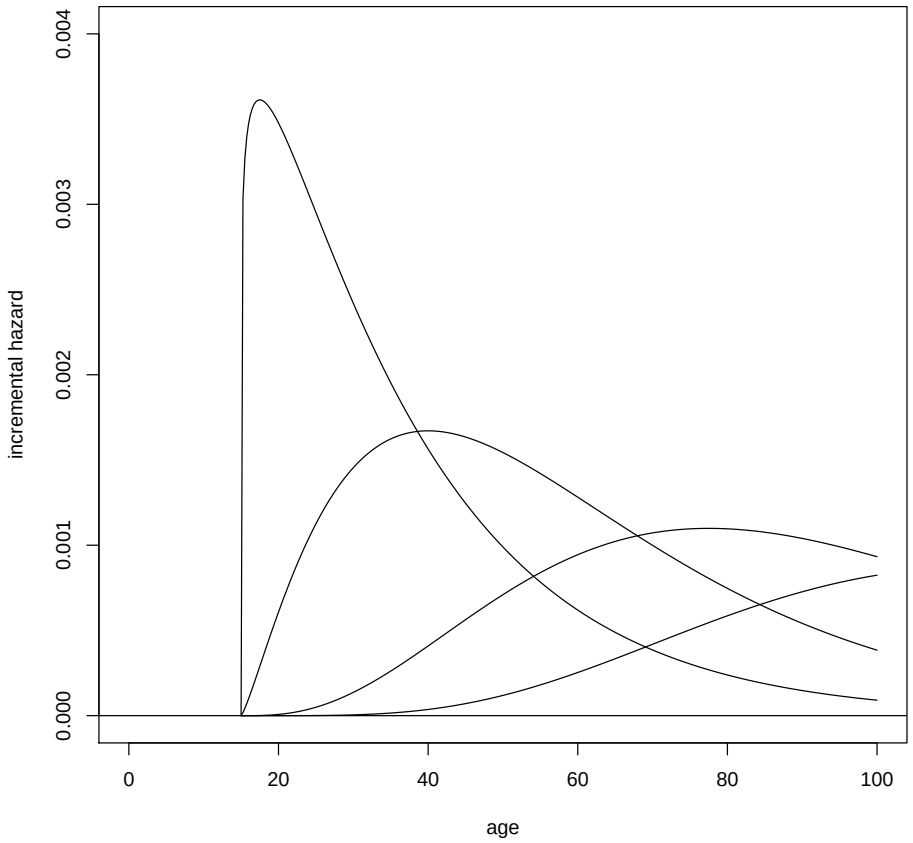

FIGURE 1. Gamma profiles for increments to the hazard function for four selected values of the mutation index m, namely 1.125, 2.250, 4.125, and 6.000, with $\alpha = 15$, $\phi = 1/20$, and $\eta = 0.100$

effect is spread over older ages, the lower is the selective cost, and the more copies there will be of m on average when natural selection manages to balance recurrent mutation. We work with cumulative hazards because of their convenient connection with lifetable survivorship functions. However, adding a multiple of a Gamma cumulative distribution function to the cumulative hazard function is the same as adding the same multiple of a Gamma density function to the hazard function itself. The mean age of action for allele m is the mean of the shifted Gamma distribution $\alpha + m/\phi$, the mode is $\alpha + (m-1)/\phi$, and the standard deviation in age of action is $\sqrt{m}/\phi$. In terms of the Gamma function Γ, the profile κ is given by

$$\kappa(m,x) = \begin{cases} \int_\alpha^x \frac{1}{\Gamma(m)} \phi^m (y-\alpha)^{m-1} e^{-\phi(y-\alpha)}\, dy, & x \geq \alpha, \\ 0, & x < \alpha. \end{cases} \tag{1}$$

Figure 1 shows the shapes of the age-specific increments to the hazard function for four typical alleles in our setting, with $\eta \equiv 0.100$, $\alpha = 15$, and m equal to 1.125, 2.250, 4.125, and 6.000.

Each member of the population carries some finite batch of mutant alleles. We use the letter g and the word "genotype" as shorthand to refer to the batch. Alleles with the same profile of action are treated as copies of the same allele even though they are found at different sites in the genome. An individual without mutant alleles has the "null genotype" $g = 0$ with wild-type alleles at every site.

The survivorship function $\ell_x(g)$ for a subpopulation of members with genotype g is the proportion of members of the subpopulation living beyond age x. To write it down, we start with an exogenous baseline cumulative hazard $\Lambda(x)$ and add to it a term $\eta(m)\kappa(m, x)$ for each m in the batch g to obtain the cumulative hazard. We multiply the cumulative hazard by -1 and apply the exponential function to obtain the survivorship.

We write capital G for the random batch of mutant alleles carried by an individual selected at random from the population. The count of alleles in G with values of m in some interval of $\mathcal{M}$ is thus a random variable. An example would be the count of alleles with shape parameters between 1 and 1.5. The mean of this random variable (which is just the population average number of mutant alleles in the interval $(1, 1.5)$) is given by the area within the interval $(1, 1.5)$ under a curve ρ called the *intensity* of G.

The intensity alone may not provide a complete description of the population's genetics: the function ρ only specifies for each region of $\mathcal{M}$ the population average number of mutant alleles in that region and *a priori* does not enable one to compute the proportion of the population that have more than some number of mutant alleles in a given region of $\mathcal{M}$ or to determine whether a randomly chosen individual who happens to have larger than expected numbers of mutant alleles in one region is more or less likely to have a larger than expected number in another region. In this model, there is a distribution of genotypes, which are batches of mutant alleles from $\mathcal{M}$; the intensity only describes the overall frequency of each mutation, with no information about its genetic partners.

When selective costs are linear — effectively, the *non-epistatic* case in which distinct loci evolve independently — the genotype distribution is a *Poisson random measure*, a mathematical construct whose properties are described, for instance, in Kallenberg (1983). Intuitively, the genotype of an individual sampled at random from the population can be described by going through $\mathcal{M}$ point by point, and taking mutations independently at random with probabilities governed by ρ. When the selective cost is nonlinear, though, there will be a complex structure of interactions between mutations.

It is surprising, then, that the simple Poisson structure returns, regardless of the complexity of the epistasis, in the Free Recombination model, as shown in Evans et al. (2007). While distinct loci now do not evolve independently, the distribution at any given time *does* have a Poisson random measure structure and is completely described by the intensity alone.

We have introduced two of the essential ingredients for specifying the model: the mutation space $\mathcal{M}$, and the translation of genotypes into mortality profiles. The next element of the specification is a mutation rate ν, which like ρ is a nonnegative

function on $\mathcal{M}$, determining the rate at which different mutations arise spontaneously. Except when we indicate otherwise, we take the mutation rate to have constant value $\nu_{tot}/(\xi - 1)$ for m in some interval $[1, \xi]$ and to be zero for $m > \xi$.

The model is a model in continuous time. As shown in Evans et al. (2007), it can be regarded as a limiting case of discrete-generation models in the limit of weak selection and mutation. It is convenient to scale the time axis so that one unit of time in the continuous-time model corresponds to one generation in discrete settings. The rate ν is then expressed in units of mutations per generation.

The final ingredient of model specification is the selective cost of a batch of mutations. We assume that mutations affect an individual's fitness only through their effect on mortality rates, and that the cumulative mortality effects of multiple mutations are additive. As discussed in Wachter et al. (2008), there are good reasons for identifying the selective cost of a batch of mutations g with the resulting lifetime loss of net reproduction:

$$S(g) := \int f_x \, \ell_x(0) \, dx - \int f_x \, \ell_x(g) \, dx \tag{2}$$

Here f_x is age-specific fertility at age x.

We take fertility to be 0 below the age of maturity α and to equal a non-zero constant above α up to a latest age at reproduction β. The value of the constant is tuned to produce an overall stationary population size. The baseline survival probability $\ell_x(0) = \exp(-\Lambda(x))$, (the survival probability when $g = 0$), is equal to $\exp(-\lambda(x - \alpha))$ for $x > \alpha$ and equal to 1 for $x \leq \alpha$. It represents the minimum realizable rate at the given age, which may be identified with the so-called the *extrinsic mortality rate*. (For a discussion of some problems inherent in the notion of extrinsic mortality rate, see Williams and Day (2003).)

The goal is to determine the intensity $\rho(m)$ of mutations at equilibrium and the corresponding expected (aggregate) population survival curve $\mathbb{E}_\rho [\ell_x(G)]$, the proportion of the whole population living beyond age x. The general formulas assuming Free Recombination are given in Evans et al. (2007). Section 3 in Wachter et al. (2008) shows that these general formulas imply in our special setting that $\mathbb{E}_\rho [\ell_x(G)]$ is given by

$$\mathbb{E}_\rho [\ell_x(G)] = \ell_x(0) \exp\left(- \int (1 - e^{-\eta \, \kappa(m,x)}) \, \rho(m) \, dm \right) \tag{3}$$

The slope of minus the logarithm of the left-hand side is the population hazard. The increment to the cumulative population hazard due to the accumulation of copies of allele m can be written

$$H(m, x) = (1 - e^{-\eta \, \kappa(m,x)}) \, \rho(m) \tag{4}$$

In this way the left-hand side of (3) takes the form $\ell_x(0) \exp(- \int H(m, x) dm)$.

The equilibrium intensity ρ has to satisfy

$$0 = \nu(m) - \rho(m) \int (1 - e^{-\eta \kappa(m,x)}) \, f_x \mathbb{E}_\rho [\ell_x(G)] \, dx \tag{5}$$

The equation (5) can be solved numerically by an iterative scheme. We start out with $\rho_0 \equiv 0$, corresponding to the null genotype and, supposing we have already constructed the approximate solutions $\rho^0, \ldots, \rho^n$, define ρ^{n+1} by

$$\rho^{n+1}(m) := \nu(m) \Big/ \left[\int (1 - e^{-\eta \kappa(m,x)}) \, f_x \mathbb{E}_{\rho^n} [\ell_x(G)] \, dx \right]. \tag{6}$$

Under appropriate conditions, it is possible to prove that this sequence does in fact converge to a solution of (5). For our numerical calculations, we approximate the continuous range of values of m by a grid with one thousand points and evaluate integrals over age by a grid with steps of 0.10 years. Calculations are implemented in the open-source R Statistical System based on the computer system S developed at Bell Laboratories.

For our numerical calculations, we approximate the continuous range of values of m by a grid with one thousand points and evaluate integrals over age by a grid with steps of 0.10 years.

4. Predictions

We now examine predicted hazard functions at mutation-selection equilibrium when the age-specific action of mutant alleles takes the form of Gamma profiles described in Section 3. We begin with a case chosen to serve as a standard example, to which we shall compare other cases. It is illustrated in Figure 2.

For our standard example, we set the baseline mortality level $\lambda = 1/20$, the rate parameter $\phi = 1/20$, the upper cutoff on shape parameters $\xi = 6$, the total mutation rate $\nu_{tot} = 0.150$, and the effect size η constant at 0.100. The maximum increment at any one age associated with our Gamma profiles is then a little more that three per thousand per year. For the sake of analogy with human life history, we set the age of initial reproduction (also the age of earliest action of the mortality profiles) to be $\alpha = 15$, and the age at end of reproduction to be $\beta = 50$.

Figure 2 shows the population hazard rate calculated from (3). It rises slowly from the background level and then accelerates, giving the impression of a Gompertz-Makeham curve in the middle of the age range, and straightening out at older ages. About one in ten-thousand individuals survive beyond age 70.

In this illustration, the equilibrium density of mutations ρ turns out to be closely approximated by an exponential function of the shape parameter, namely $\rho(m) \approx 0.170 \exp(1.377\, m)$. On average, individuals in the population carry about two mutant alleles with $m < 2.0$, a bit over a dozen with $3.5 < m < 4.0$, and nearly three-hundred with $5.5 < m < 6.0$, for an average total of 526. The Poisson standard deviation of the total number of alleles across individuals is around 20.

The effect for a given m peaks at age $15 + (m - 1)/\phi$. The effects for $m < 2.0$ are peaking before age 35, an age to which most members of the population survive. The cost in net reproduction from an additional mutation affecting these ages is high, and selection keeps their equilibrium representation low. Effects for $m > 5.5$ only become substantial at ages at which most individuals have already died. Selective costs are low and copies persist long enough to be found at high numbers in the population despite the rarity of new mutations.

Figure 3 shows the logarithm of the population hazard rate for three comparative cases. The standard example is the solid curve. The dotted curve has $\nu_{tot} = 0.170$ and an upper shape parameter cutoff of $\xi = 5.5$. The dashed curve has $\nu_{tot} = 0.120$ and $\xi = 7$. These alternatives have been chosen from among cases for which the hazard is between 0.300 and 0.550 at the age to which one in ten thousand survive, respectively equal to 69.9, 71.9, and 66.7 years.

The higher hazards at old ages in the dotted curve are due to the presence of later-acting alleles with m ranging up to 7. These alleles have effects whose age-specific profiles increase throughout the range of ages to which population members

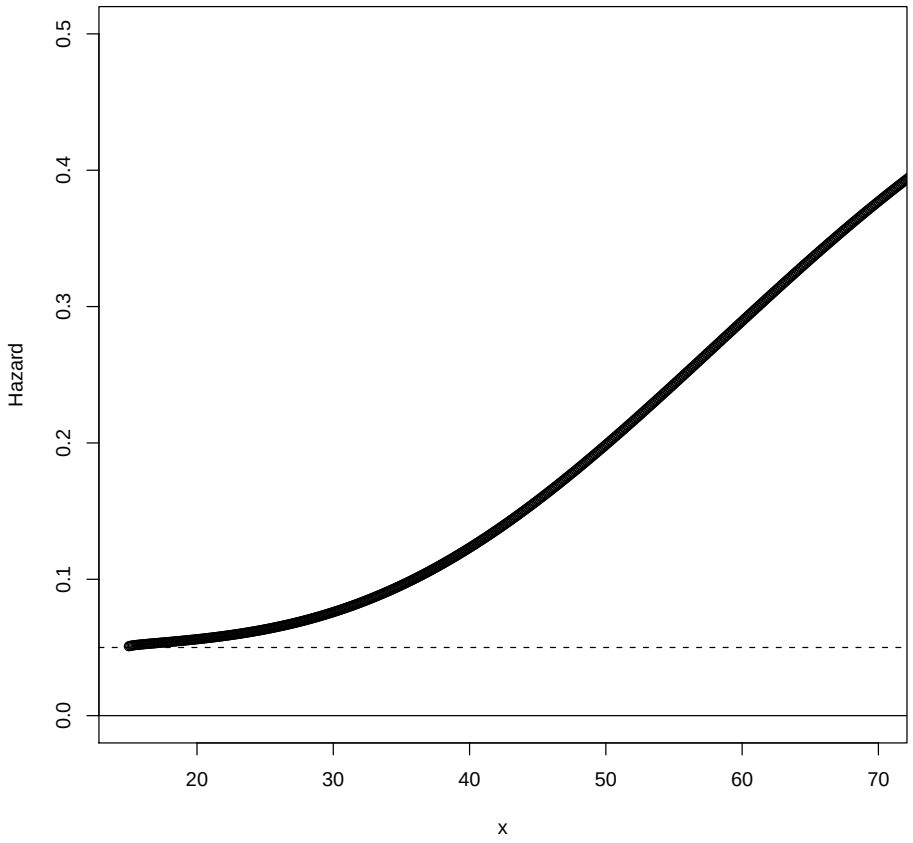

FIGURE 2. Predicted hazard for a standard example with $\lambda = \phi = 1/20$, $\nu_{tot} = 0.150$, $\xi = 6$, $\alpha = 15$, and $\beta = 50$

survive. The mode for $m = 7$ is not reached until 135 years. Although the mutation rate is less for the dotted curve, the shapes of the age-specific effects lead to higher hazards toward the end of life.

We see that mutation accumulation with the given profiles and parameters produces a long middle stretch of nearly loglinear hazards, corresponding to a Gompertz form. At young ages the curves are convex on the logarithmic scale, bending upward, as effects of mutant alleles come into play. At older ages, the curves turn concave. Accumulation of mutational effects concentrated at late ages is held in check by their small accompanying effects at young ages in this specification.

The interactions among effects at different ages taken into account by the nonlinear model turn out to have a substantial impact on predictions, as expected from results in Wachter et al. (2008). We compare predictions from the full non-linear model to predictions from a linear approximate model of the kind on which earlier studies have relied. Figure 4 shows the population survivorship function for our

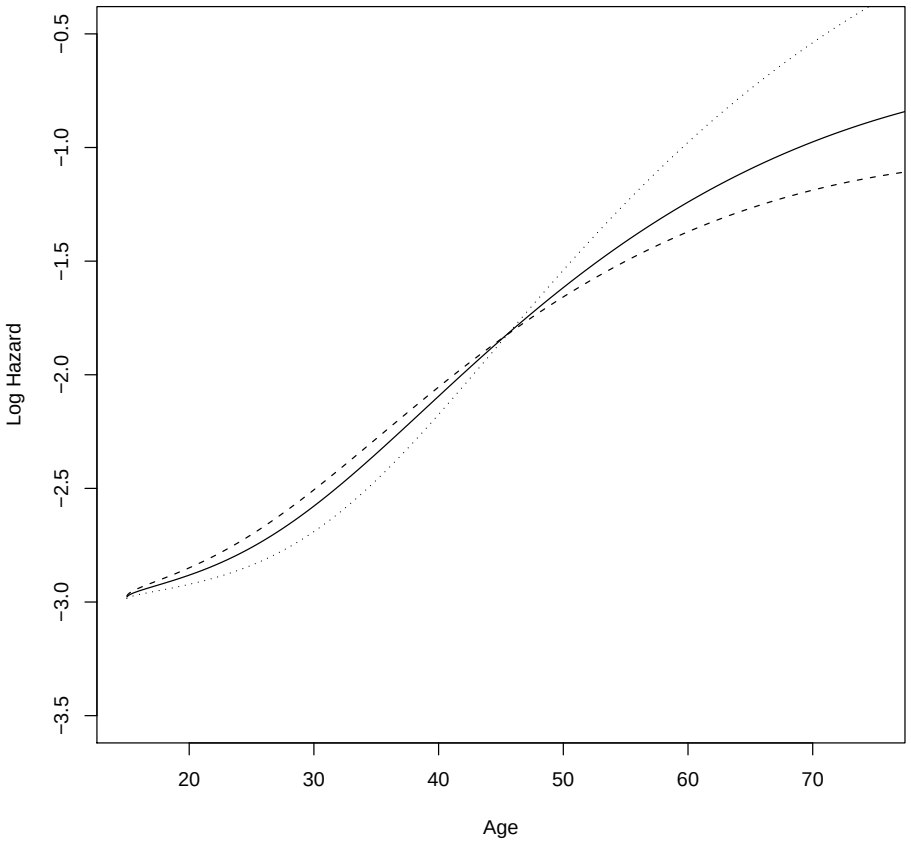

FIGURE 3. Logarithm of predicted hazard for three cases showing early upward bend, straight middle Gompertzian stretch, and late downward bend. The cases all have $\lambda = \phi = 1/20$ and $\eta \equiv 0.100$. The solid curve has $\nu_{tot} = 0.150$, and $\xi = 6.0$; the dashed curve has $\nu_{tot} = 0.170$, and $\xi = 5.5$; the dotted curve has $\nu_{tot} = 0.120$, and $\xi = 7.0$.

standard example in a thick line, along with baseline survivorship in a dashed line, and survivorship from the linear approximate model between them in a dotted line. Only about a third of the reduction in life expectancy from 35.0 years to 28.8 years due to mutation accumulation is captured by the linear approximate model.

The sizes of effects, in contrast to their shapes, turn out to have only modest influence on the predictions. Alleles with smaller effects accumulate at equilibrium in greater numbers. Changes in the intensity ρ roughly balance changes in effect size η. Figure 5 shows the predicted hazard functions with parameters taken from our standard example but with difference choices of η.

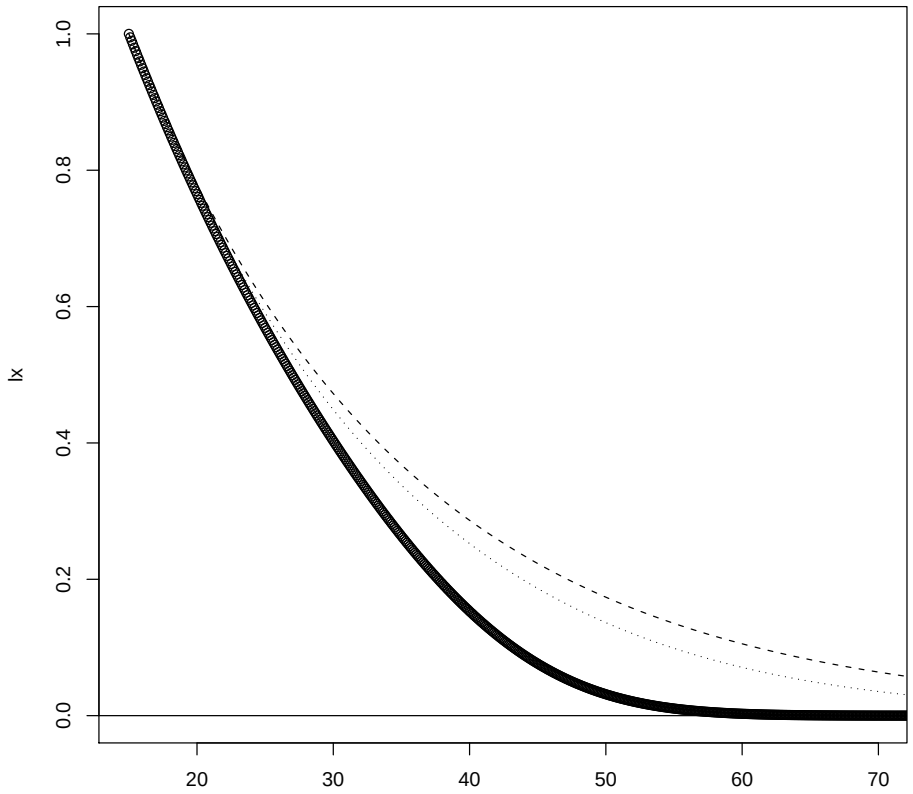

FIGURE 4. Probability of survival by age for the standard example as predicted by the full non-linear model (circles), by a linear approximate model (dots), and by the baseline model

Three uppermost curves, almost indistinguishable, have constant $\eta = 0.0001$, $\eta = 0.001$, and $\eta = 0.010$. The mean total number of mutant alleles runs to a bit over five hundred thousand in the first case, fifty-thousand in the second, and five thousand in the third. Three slightly lower curves, also hardly distinguishable, include our example with η constant at 0.100 and two examples with changing η, one rising linearly with the shape parameter from 0.020 to 0.200 and one falling linearly from 0.200 to 0.020. Mean counts of alleles are 527, 309 and 1493 respectively. Small effect sizes accompany larger mean numbers when they occur for alleles with late action. The lowermost curve has $\eta = 1.000$ and a mean of only 51 alleles. Only as η becomes this large, outside the range of intended application of the model, do we see substantially different predicted hazard functions.

The approximate invariance of predicted hazard functions with effect sizes is an expression of Haldane's Principle, enunciated by Haldane (1937) and discussed in

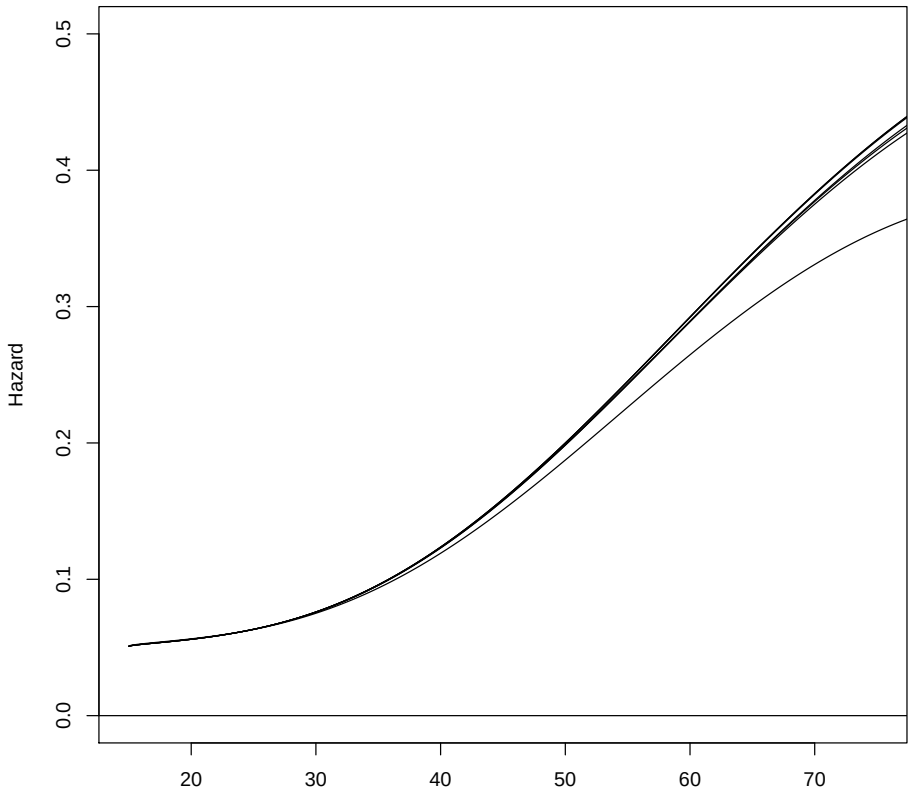

FIGURE 5. The influence of effect size is shown with predicted hazard functions from seven cases described in the text, some with indistinguishable outcomes, sharing all parameter values except effect size with the example of Figure 1

terms of our non-linear models in Wachter et al. (2008). In Equation (4), the contribution $H(m, x)$ from allele m is nearly linear in $\eta(m)\rho(m)$ for small η, so scaling $\eta(m)$ up can be nearly compensated, allele by allele, by scaling $\rho(m)$.

One of the most familiar general predictions of the evolutionary theory of senescence is a positive relationship between the level of background or extrinsic mortality associated with risks of predation in natural settings and the "rate of senescence" measured by the slope of the logarithm of the hazard rate with respect to age. Our predictions hint at such a relationship, but only for substantial values of the baseline hazard λ. Figure 6 shows the logarithms of the predicted equilibrium hazard for our standard set of parameters as the level of the constant baseline hazard is raised from 0.020 to 0.050 and on to 0.080.

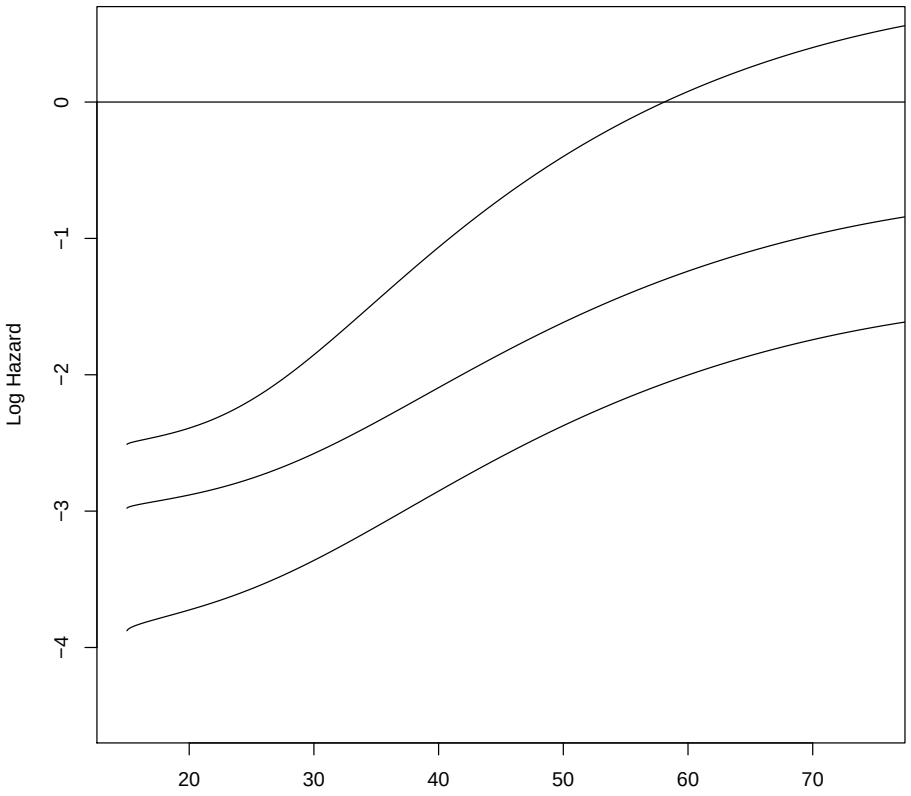

FIGURE 6. The influence of the level of extrinsic hazards on the pace of senescent mortality is shown by predicted log hazards from three cases sharing parameters with the standard example of Figure 1 except for λ, which ranges, from bottom to top, over values 0.020, 0.050, and 0.080

Slopes computed over the middle range of ages from 30 to 50 to which a Gompertz fit is roughly hover around 0.050 for the first two cases but rise to 0.074 as λ increases to 0.080. In cases not shown here in which non-zero fertility extends to higher ages, there is a closer match between values of the slope and values of the parameter λ itself, paralleling a relationship found with linear approximate models in Charlesworth (2001).

The stretch of ages with exponentially increasing hazards, corresponding to linear increase in log hazards, visible in Figures 2 and 3 does not extend out to extreme ages. Attenuation of increase is already visible in the upper ages toward right of those figures. We focus on this attenuation in Figure 7, which shows the predicted hazard rate for the same standard example of Figure 2 but with a horizontal axis

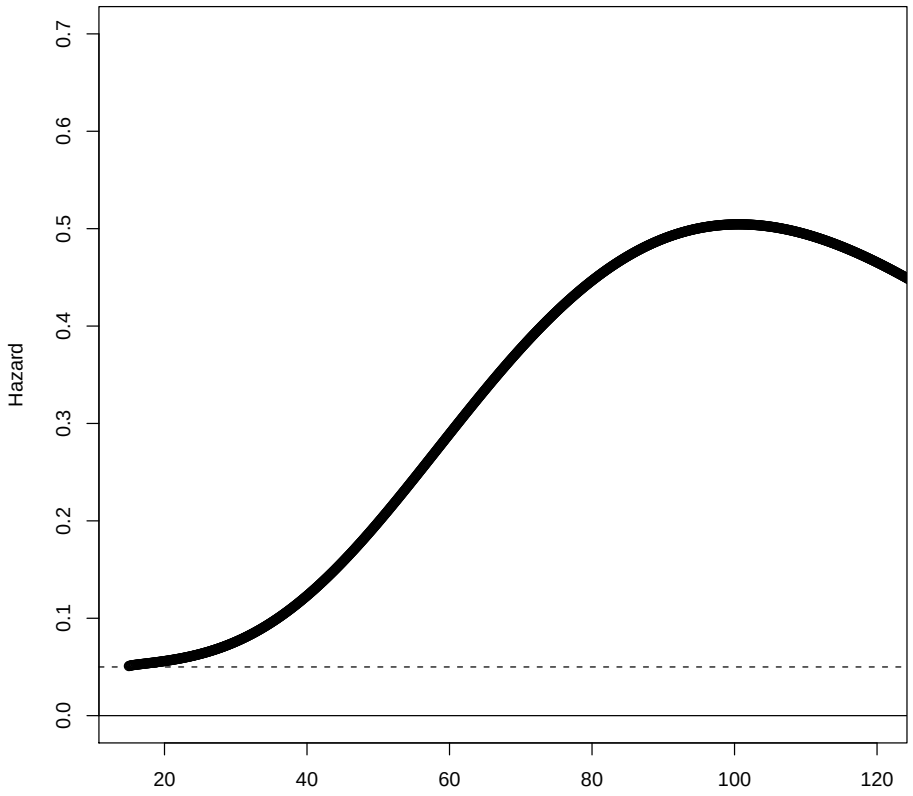

FIGURE 7. A plateau in the predicted hazard function at extreme ages in the standard example of Figure 2 with a longer range of ages.

extending all the way out to an age of 120 years. The vertical scale also differs from Figure 2. Around 100 years, the hazard levels off, establishing a brief plateau phase, and by 120 years a declining hazard is apparent. Only one in ten billion survive to 100 years with our standard parameter choices, but the plateau and subsequent decline are to be expected with parameters leading to milder mortality regimes as well.

The plateau at extreme ages is due to the property of the profiles for the age-specific action of mutant alleles to which we have already called attention, namely that even alleles whose action is spread over old ages all have some small effects at young ages. These small effects rein in the accumulation of late-acting mutant alleles. They prevent any Wall of Death; that is, any finite age at which the hazard rate goes to infinity and survivorship reaches zero. Walls of Death occur in many elementary cases for profiles with Hamilton-style, point-mass profiles, as shown in

Wachter et al. (2008). The proposal for generating plateaus by assuming some small effects at young ages for all mutant alleles was put forward by Charlesworth (2001) and shown to be valid for the linear approximate model. We now see that these outcomes also hold in the full non-linear model with the particular profiles we are studying.

In summary, we have found that the process of mutation accumulation can readily produce predicted population hazard functions with the chief features highlighted by the cross-species comparisons of biodemographers. It can produce a stretch of ages with an exponential, Gompertzian rise in hazards and it can produce a late-age hazard plateau. These outcomes arise from a set of assumptions about the age-specific action of mutant alleles that are suggested by examples from reliability theory and from the functional approach to the study of senescence. It remains, however, to develop comprehensive models in which the generic mutation accumulation machinery is driven by plausible genetic and physiological mechanisms, and in which age-specific tradeoffs are derived compellingly from reliability theory. It also remains to be determined whether the examples studied here are typical, or whether they represent peculiar outcomes of our specific choices of parameter values. More generally, the field is open for attempts to characterize the conditions under which the force of natural selection in the presence of recurring deleterious mutation will mold hazard functions into familiar forms.

References

[1] Bürger R (2000) The mathematical theory of selection, recombination, and mutation. John Wiley, Chichester, New York

[2] Campisi J (2003) Cellular senescence and apoptosis: how cellular responses might influence aging phenotypes. Experimental Gerontology 38(1):5–11

[3] Carey JR (2003) Longevity: The Biology and Demography of Life Span. Princeton University Press

[4] Carey JR, Tuljapurkar S (eds) (2003) Life Span: Evolutionary, Ecological, and Demographic Perspectives. Population Council, pop. Dev. Rev. vol. 29 suppl

[5] Charlesworth B (1994) Evolution in age-structured populations. Cambridge University Press, Cambridge

[6] Charlesworth B (2001) Patterns of age-specific means and genetic variances of mortality rates predicted by the mutation-accumulation theory of ageing. J Theor Bio 210(1):47–65

[7] Evans SN, Steinsaltz D, Wachter KW (2007) A mutation-selection model for general genotypes with recombination, http://arxiv.org/abs/q-bio.PE/0609046

[8] Finkelstein M, Esaulova V (2006) Asymptotic behavior of a general class of mixture failure rates. Advances in Applied Probability 38(1):244–62

[9] Gavrilov LA (1978) A mathematical model of the aging of animals. Doklady Akademii Nauk SSSR 238:490–2

[10] Gavrilov LA, Gavrilova NS (1991) The Biology of Lifespan: A Quantitative Approach. Harwood Academic Publishers, Chur, Switzerland

[11] Gavrilov LA, Gavrilova NS (2001) The reliability theory of aging and longevity. Journal of Theoretical Biology 213:527–45

[12] Haldane JBS (1937) The effect of variation on fitness. American Naturalist 71:337–49

[13] Hamilton WD (1966) The molding of senescence by natural selection. J Theor Bio 12:12–45

[14] Hasty P (2001) The impact energy metabolism and genome maintenance have on longevity and senescence : lessons from yeast to mammals. Mechanisms of Ageing and Development 122(15):1651–62

[15] Hedrick PW (1999) Antagonistic pleiotropy and genetic polymorphism: a perspective. Heredity 82:126–33

[16] Kallenberg O (1983) Random measures. Academic Press, New York

[17] Kimura M, Maruyama T (1966) The mutational load with epistatic gene interaction. Genetics 54:1337–51
[18] Medawar P (1952) An unsolved problem in biology: An inaugural lecture delivered at University College, London, 6 December, 1951. H. K. Lewis and Co., London
[19] Nyström T (2003) Conditional senescence in bacteria: death of the immortals. Molecular Microbiology 48(1):17–23
[20] Pletcher SD, Neuhauser C (2000) Biological aging — criteria for modeling and a new mechanistic model. International Journal of Modern Physics C 11(3):525–46
[21] Rose MR (1985) Life history evolution with antagonistic pleiotropy and overlapping generations. Theoretical Population Biology 28(3):342
[22] Rosen R (1978) Feedforwards and global system failure: A general mechanism for senescence. Journal of Theoretical Biology 74:579–90
[23] Schnebel EM, Grossfield J (1988) Antagonistic pleiotropy: An interspecific Drosophila comparison. Evolution 42(2):306–11
[24] Steinsaltz D, Evans SN, Wachter KW (2005) A generalized model of mutation-selection balance with applications to aging. Adv Appl Math 35(1):16–33
[25] Strehler B, Mildvan A (1960) General theory of mortality and aging. Science 132(3418):14–21
[26] Toupance B, Godelle B, Gouyon PH, Schächter F (1998) A model for antagonistic pleiotropic gene action for mortality and advanced age. The American Journal of Human Genetics 62(6):1525–34
[27] Vaupel JW, Carey JR, Christensen K, Johnson TE, Yashin AI, Holm NV, Iachine IA, i VK, Khazaeli AA, Liedo P, Longo VD, Zeng Y, Manton KG, Curtsinger JW (1998) Biodemographic trajectories of longevity. Science 280(5365):855–60
[28] Wachter KW (1999) Evolutionary demographic models for mortality plateaus. Proceedings of the National Academy of Sciences, USA 96:10,544–7
[29] Wachter KW, Finch CE (eds) (1997) Between Zeus and the Salmon: The Biodemography of Longevity. National Academy Press, Washington, D.C.
[30] Wachter KW, Evans SN, Steinsaltz DR (2008) The age-specific force of natural selection and walls of death, under review, http://arxiv.org/abs/0807.0483
[31] Weitz J, Fraser H (2001) Explaining mortality rate plateaus. Proceedings of the National Academy of Sciences, USA 98(26):15,383–6
[32] Williams GC (1957) Pleiotropy, natural selection, and the evolution of senescence. Evolution 11:398–411
[33] Williams PD, Day T (2003) Antagonistic pleiotropy, mortality source interactions, and the evolutionary theory of senescence. Evolution 57(7):1478–88

Department of Demography, University of California, Berkeley, 2232 Piedmont Avenue, Berkeley, CA. 94720-2120, USA
E-mail address: wachter@demog.berkeley.edu

Department of Statistics, University of Oxford, 1 South Parks Road, Oxford, Oxfordshire, OX13TG, UNITEED KINGDOM
E-mail address: david.steinsaltz@stats.ox.ac.uk

Department of Statistics, University of California, Berkeley, 367 Evans Hall, Berkeley, CA. 94720-3860, USA
E-mail address: evans@stat.berkeley.edu